Schifferle, L., Speziale, S., Lobanov, S. S. (2022): High-pressure evolution of the refractive index of MgO up to 140 GPa. - Journal of Applied Physics, 132, 125903.

https://doi.org/10.1063/5.0106626

Journal of Applied Physics ARTICLE scitation.org/journal/jap

High-pressure evolution of the refractive index of MgO up to 140 GPa

Cite as: J. Appl. Phys. **132**, 125903 (2022); doi: 10.1063/5.0106626
Submitted: 29 June 2022 · Accepted: 31 August 2022 ·
Published Online: 28 September 2022

View Online Export Citation CrossMark

Lukas Schifferle,[1,2] Sergio Speziale,[1] and Sergey S. Lobanov[1,2,a)]

AFFILIATIONS

[1]GFZ German Research Center for Geosciences, Telegrafenberg, 14473 Potsdam, Germany
[2]Institute of Geosciences, University of Potsdam, Karl-Liebknecht-Straße 24-25, 14476 Potsdam, Germany

[a)]**Author to whom correspondence should be addressed:** slobanov@gfz-potsdam.de

ABSTRACT

Refractive index provides fundamental insights into the electronic structure of materials. At high pressure, however, the determination of refractive index and its wavelength dispersion is challenging, which limits our understanding of how physical properties of even simple materials, such as MgO, evolve with pressure. Here, we report on the measurement of room-temperature refractive index of MgO up to ~140 GPa. The refractive index of MgO at 600 nm decreases by ~2.4% from ~1.737 at 1 atm to ~1.696 (±0.017) at ~140 GPa. Despite the index at 600 nm is essentially pressure independent, the absolute wavelength dispersion of the refractive index at 550–870 nm decreases by ~28% from ~0.015 at 1 atm to ~0.011 ($\pm 8.04 \times 10^{-4}$) at ~103 GPa. Single-effective-oscillator analysis of our refractive index data suggests that the bandgap of MgO increases by ~1.1 eV from 7.4 eV at 1 atm to ~8.5 (±0.6) eV at ~103 GPa.

I. INTRODUCTION

Refractive index is a fundamental material property that reflects the response of electric charges in the material to the oscillating electromagnetic field. The pressure dependence of the refractive index (n) and its wavelength dispersion in the near-infrared (near-IR), visible (VIS), and ultraviolet (UV) regions are of great interest as they give insights into the effects of pressure on the electronic band structure of materials upon compression.[1] For example, refractive index and its dispersion allow correlations with structural properties such as coordination number and chemical bond character.[2,3] The change of refractive index with pressure is also of direct importance to geophysics because radiative thermal conductivity, which is believed to increase with depth in the Earth, is proportional to n^2.[4,5] Furthermore, refractive index of materials at high pressure allows the determination of diamond–diamond separation in diamond anvil cell (DAC) experiments, which in turn is a key parameter needed to determine thermal/electrical conductivities of materials in DAC experiments. The existent large discrepancy in the thermal conductivities of the Earth's mantle and core,[6–15] based on DAC experiments, may be rooted in the inadequate assessment of samples' thickness at high pressure. Finally, the density dependence of the refractive index is also needed in shockwave experiments where n of the interferometer window is essential for velocity corrections needed to determine the properties of the sample.[16]

MgO, a simple oxide crystallizing in the rock salt structure (B1), has attracted a high number of experimental and theoretical studies because it is a prototypical ionic oxide of technological importance[17] and relevance as a planetary building block.[18,19] The stability of MgO at high temperature (T) (melting point 3098 K)[20] and its chemical inertness make it suitable for industrial applications as a refractory material.[17,21] At $T < 3000$ K, B1 MgO is also stable to very high pressures (P) (up to > ~400 GPa).[18,22–24] The abundance of Mg and O in planetary-forming environments and the P–T stability of MgO render it a material of special interest to geo- and planetary scientists. In particular, the physical properties of MgO at high P–T conditions are needed to model planetary dynamics.[18,19] MgO is also frequently used in high-pressure experiments[25–27] as a chemical/thermal insulator and as a pressure calibrant,[28] due to its physical stability and a well-established equation of state (EOS).[22,29,30] Although the physical properties of MgO at high pressure have been the subject of many studies, its optical properties, which are of both practical and fundamental importance, remain poorly constrained.

Information on the refractive index of MgO at high pressure ($P > 30$ GPa) is limited to (a) a single density-functional theory

(DFT) computation[30] of the high-frequency dielectric constant (ϵ_∞), where $n = \sqrt{\epsilon_\infty}$ and (b) shockwave experiments that inferred the index of MgO in the near-IR range.[31] Both studies are broadly consistent with each other and show that the electronic contribution to the index of MgO decreases upon compression to 100 GPa by ~2%–4%. Direct measurements of the refractive index of MgO at constant temperature[16,32,33] are limited to pressures below 23 GPa.[16] The wavelength dispersion of the refractive index of MgO at high pressure is also unknown. Here, we report on the room-temperature refractive index of MgO in the VIS and near-IR to ~140 GPa and its wavelength dispersion to ~103 GPa. These data provide the first experimental constrain on the evolution of the bandgap of MgO at high pressures. Furthermore, we show that the refractive index of MgO reported here allows quantitative optical measurements of sample thickness and volume, which can be used in experiments to determine the density of non-crystalline solids at high pressure.

II. EXPERIMENTAL METHODS

A. Sample and preparations

High-pressure experiments were performed using symmetric DACs equipped with pairs of matching diamonds with culet sizes of 300/100 μm (beveled) and 400 μm (flat). Rhenium gaskets indented between the diamond anvils to a thickness of 10–25 μm were laser-drilled to create cylindrical holes with diameters of ~45 μm (for 300/100 μm anvils) and ~190 μm (for 400 μm anvils) to serve as sample chambers. For each loading, we used a freshly cleaved piece of MgO with dimensions to fully fill the sample chamber. After placing the MgO sample without any pressure transmitting medium, we immediately closed the DAC to minimize sample contamination by atmospheric moisture. Increasing the pressure to ~20 GPa was sufficient to obtain an optically homogenous sample, which is necessary for the refractive index measurements.[34–36] Pressure was determined by measuring the shift of the high-frequency edge of the first-order Raman band of diamond with a relative uncertainty in pressure of ~5%.[37]

B. Refractive index measurements at 600 nm

To measure the refractive index at high pressure, we use the optical reflectivity method.[34,35] For a perpendicularly incident light probe, the reflectivity of the diamond–sample interface ($R_{dia-smp}$) is related to the refractive indices of diamond (n_{dia}) and sample (n_{smp}),

$$R_{dia-smp} = \left|\frac{n_{smp} - n_{dia}}{n_{smp} + n_{dia}}\right|^2. \quad (1)$$

The probe is a broadband laser (2 W Leukos New Wave supercontinuum, 400–2400 nm) inserted into the optical path of our DAC microscope[38] by a non-polarizing beam splitter cube after passing through a shortpass (~950 nm cutoff) and a variable neutral density filter. The use of a narrow, collimated laser beam (diameter of 1.2 mm at $\lambda = 440$ nm and 2.2 mm at $\lambda = 800$ nm) and a 20× apochromatic objective allowed for a near-normal incidence of the probe and a small probe diameter in the focal plane (~5 μm). The reflected beam was passed through a spatial filter (2 × 50 mm achromatic doublets and a 75 μm confocal pinhole) and recorded on a Pixis-256E CCD, installed on a Princeton Instruments SpectraPro HRS-300-SS spectrometer (grating 300 g/mm, blaze 500 nm, wavelength calibration accuracy ~0.5 nm).

In the case of a thin (~10–25 μm) transparent sample (such as MgO) in the DAC, the reflectivity of the diamond–sample interface can be expressed as[2]

$$\frac{I_1 + I_2}{I_0} = R^3_{dia-smp} - 2R^2_{dia-smp} + 2R_{dia-smp}, \quad (2)$$

where I_0 is the probe intensity striking the upstream diamond–sample interface. I_1 and I_2 are individual reflections from the upstream and downstream diamond–sample interfaces [Fig. 1(a)]. The supplementary material of Lobanov *et al.*[2] presents derivations of Eq. (2). I_0 is obtained by measuring the amount of light reflected from a reference mirror (I_{mirror}) in the 500–800 nm range (where the reflectivity of the reference mirror is ~99%) and accounting for the light reflected from the upstream diamond–air interface. Because samples in DACs are thin, the reflected signal measured at the diamond–sample interface is a combination of I_1 and I_2 contributions. Accounting for backreflections at the diamond–sample and diamond–air interfaces, we obtain the intensity ratio spectrum ($I_{ratio} = \frac{I_1+I_2}{I_0}$). Averaging $\frac{I_1+I_2}{I_0}$ [Fig. 1(b)] over the 550–650 nm range (where the reflectivity of the reference mirror is nearly flat) allows solving Eq. (2) for $R_{dia-smp}$. Note that averaging the I_{ratio} spectrum at 550–650 nm (i.e., over a set of 370 individual intensity data due to the wavelength resolution of our system) provides a statistically more significant average than only averaging I_{ratio} at the interference pattern extrema observed at ~550–650 nm (typically, less than 20). Using $R_{dia-smp}$, we solve Eq. (1) for n_{smp} of MgO at 600 nm under the assumption of a pressure-independent refractive index of diamond ($n_{dia} = 2.418$).[20] This is a reasonable assumption as discussed by Zha *et al.*[35] and Lobanov *et al.*[2] based on the high-pressure reflectivity of a reference material and small dispersion of diamond. The refractive index of MgO reported here provides further evidence for the adequacy of this assumption, as discussed in Sec. IV. Solutions to Eqs. (1) and (2) were found using NumPy[39] and SymPy[40] Python libraries.

We also measured the refractive index of MgO at 1 atm by probing the reflectivity of the MgO–air interface of a large (~1 mm) free-standing freshly cleaved sample. Equation (1) was then modified ($n_{air} = 1$) and solved for the refractive index of MgO. We empirically estimate the apparently random error in all refractive indices of MgO reported in this work at ~±1%.[2] This estimate is based on the reproducibility of refractive indices measured at the same DAC load and sample position. Improvements on the reproducibility of sample positioning and a high-resolution tilting DAC stage as well as accurate characterization of the variation in probe intensity over the typical measurement time (~10 min) may help to reduce random variations in the measured refractive index.

C. Dispersion of the refractive index

The intensity ratio spectrum is an interference pattern because the DAC sample cavity is a Fabry–Pérot interferometer. The

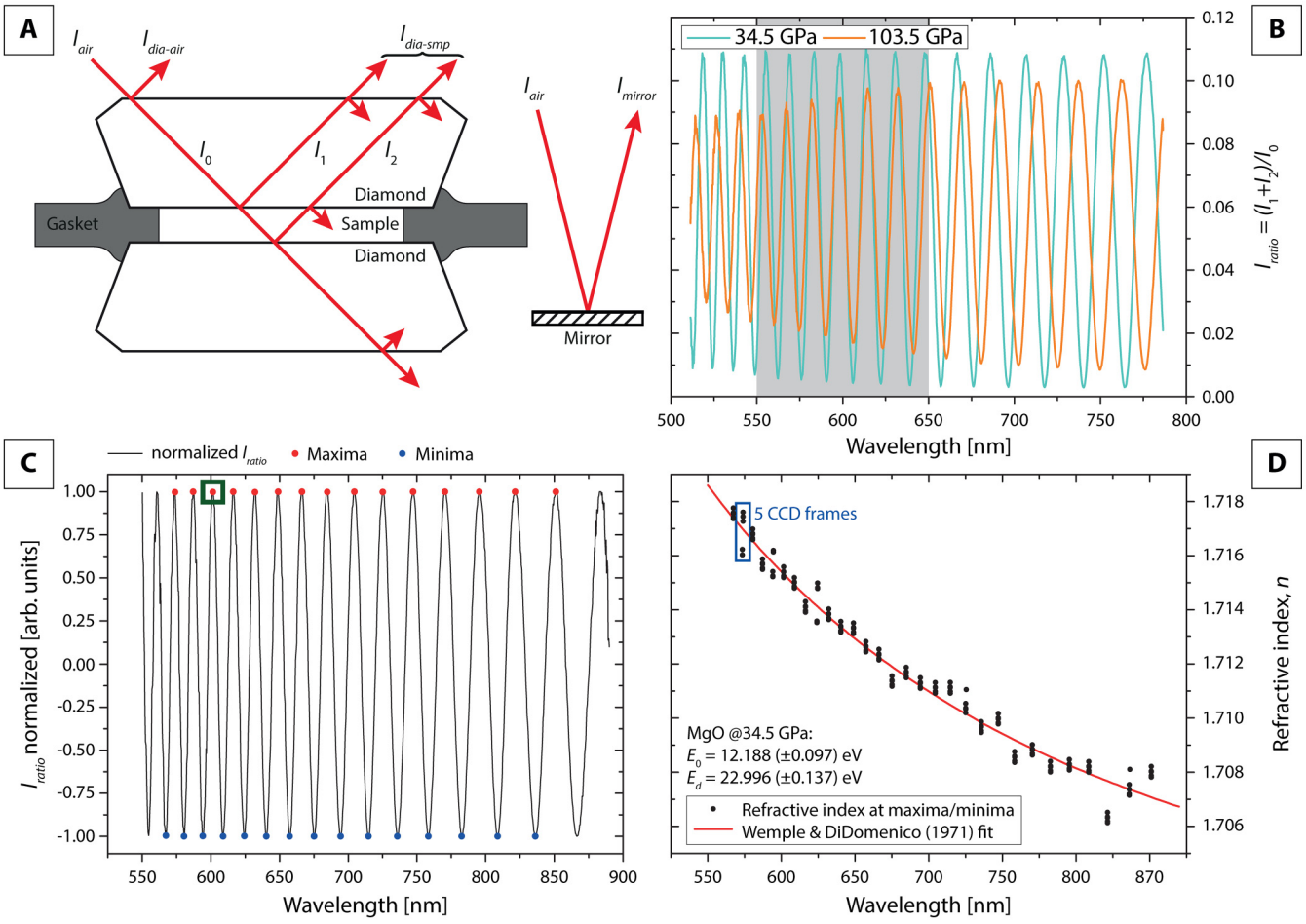

FIG. 1. (a) Reflectivity measurement in diamond anvil cell. Perpendicularly incident probe laser is partially reflected at diamond–air and diamond–sample interfaces. Oblique probe incidence is depicted for clarity. (b) Measured intensity ratio spectra (MgO run 4 at 34.5 and 103.5 GPa) are averaged over 550–650 nm (gray area) to solve Eq. (2) for $R_{dia\text{-}smp}$. The different contrast of the patterns at 34.5 and 103.5 GPa is due to diamond cupping, which has been shown to have no apparent effect on the inferred refractive index.[34] (c) Normalized intensity ratio spectrum from reflectivity measurements in a DAC (MgO run 4 at 34.5 GPa). The blue and red dots are local extrema. The green square highlights the extremum closest to 600 nm. (d) The wavelength dispersion of the MgO refractive index at 34.5 GPa and its Wemple and DiDomenico[3] single-effective-oscillator fit.

interference condition for each of the observed minima and maxima is

$$\lambda k(\lambda) = 2dn_{smp}(\lambda), \tag{3}$$

where $k(\lambda)$ is the interference order number of the extremum (in half-integer step sizes) observed at wavelength λ, d is the sample thickness, and $n_{smp}(\lambda)$ is the refractive index of the sample at the extremum. The refractive index of the sample measured at 600 nm allows analyzing the interference pattern for index dispersion. This requires, however, that chromatic aberrations due to the use of refractive optics are minimized and that the determination of extrema wavelengths is as accurate as possible. Toward this end, the reflectance spectra were also collected with a 10× apochromatic objective whose reduced numerical aperture (0.26 for 10× vs 0.4 for 20×) allows minimizing chromatic aberrations. The reflected signal was recorded by a Princeton Instruments Acton SP-2150i spectrometer (300 g/mm, blaze 750 nm) with a Pixis-100B eXcelon CCD detector, which enabled for a wavelength resolution of ~0.4 nm/pixel.

Writing Eq. (3) for any pair of extrema (e.g., at k and $k+1$) and using the index measured at 600 nm, we can estimate the sample thickness. Here, however, we obtain a more precise estimate of sample thickness by iterating through all the extrema while assuming n_{smp} is wavelength independent. The latter assumption is reasonable to first-order and contributes only a small systematic error to the thickness estimate (< ~1% of the value) because the index dispersion of MgO over the 550–870 nm range is only

~0.85% (1 atm).[41] Using the sample thickness in Eq. (3), we can now find the interference order number of the extremum closest to 600 nm [Fig. 1(c)] and then use it to assign the interference order to all the other observed extrema. Finally, we use Eq. (3) to obtain the refractive index at all the extrema using their respective interference order numbers. A repeated collection of five CCD frames at the same sample position allowed minimizing random errors in the measured index dispersion due to CCD noise [Fig. 1(d)]. To further account for small variations in the measurement position, we collected additional spectra ~2–5 μm off the central sample position. This allowed evaluating the combined random and systematic relative errors in the measured index dispersion, which are ~1.2% at 18.8 GPa and ~7.5% at 103.5 GPa. We attribute the increase in error with pressure to the expected diamond cupping at high pressure,[42,43] which introduces slight (~20–40 nm) wavelength-dependent differences in the optical path length ($n_{smp}d$) of the probe in the DAC sample due to the wavelength-dependent beam diameter of the light probe (due to the light source characteristics and unavoidable chromatic aberration).

D. Measurements of sample thickness, area, and volume

Sample thickness at the center of the sample chamber was determined using the refractive index of MgO at 600 nm. Due to diamond cupping, expected at high pressure, we also measured the sample thickness at the periphery of the sample at four distinct locations ~5 μm from the gasket edge. The averaged sample thickness at the periphery (d_{edge}) and at sample center (d_{center}) was then used to evaluate the mean sample thickness (d_{mean}). To measure the area (A) of the sample, we analyzed images of both sides of the DAC recorded by a FLIR Blackfly BFS-U3-50S5C-C camera (1 px $\approx 0.013\,\mu m^2$) and calculated the average. All images were taken at fixed back-illumination conditions and analyzed using ImageJ[44] by converting the image into an 8-bit gray scale and finding all the pixels with brightness higher than a threshold (value: 61). These measurements allowed us to derive the absolute volume ($V = A \cdot d_{mean}$) of MgO samples as a function of pressure. As was shown by Lobanov *et al.*,[2] this approach is sufficient to achieve relative errors of ~1.5% for A that propagate together with the error in d_{mean} to an ~3% error in V.

III. RESULTS

The refractive index of MgO at 600 nm decreases with pressure by ~2.4% from ~1.737 at 1 atm to ~1.696 (±0.017) at ~140 GPa (Fig. 2). The index at 600 nm measured here is ~1% higher than that determined in shockwave experiments of Fratanduono *et al.*[31] at 1550 nm. This difference is consistent with the decrease in the refractive index of MgO by ~1.2% from 600 to 1500 nm at 1 atm.[41] Our results are also in agreement with the local-density approximation (LDA) DFT calculations of Oganov *et al.*[30] but the computed index is systematically higher than that measured in experiments, likely due to the tendency of LDA-DFT to underestimate the bandgap.[45]

Both sample thickness and area decrease with increasing pressure (Fig. 3). Diamond cupping is evident as the sample thickness near the gasket edge is systematically smaller than the thickness at

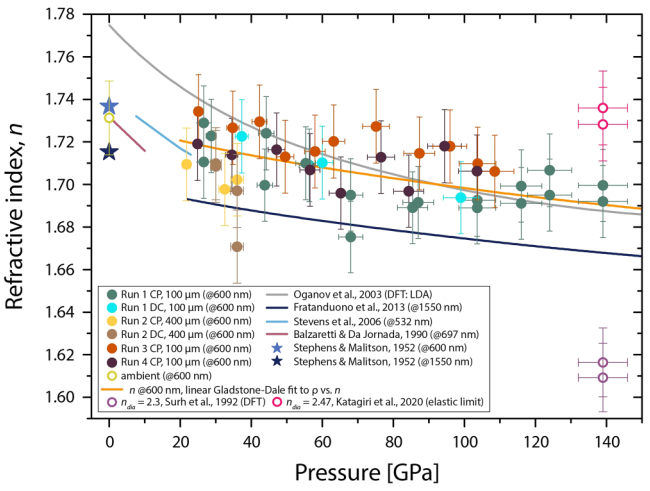

FIG. 2. The refractive index of MgO at 600 nm measured in this work (circles, where CP = compression, DC = decompression) compared to shock wave data at 1550 nm[31] (dark blue curve, with uncertainties as large as 1% of the measurements) and at 532 nm (light blue curve), interferometry measurements (rose curve)[33] and computations by Oganov *et al.*[30] (gray curve). Orange line is $n(P)$ based on the linear Gladstone–Dale fit using experimental n and ρ from Tange *et al.*[29] The refractive index at 1 atm is after Stephens and Malitson[41] and is shown by light blue (at 600 nm) and dark blue (1550 nm) stars. Violet and pink open circles are MgO refractive indices obtained by assuming $n_{dia} = 2.3$[46] and $n_{dia} = 2.47$.[47]

sample center at $P > 30$–40 GPa, consistent with previous measurements of diamond–diamond separation in DAC experiments.[2,42,43] We observe a maximum relative difference of ~2% between center and periphery as well as an overall thinning of the sample by ~14% from ~19 to ~103 GPa. The evolution of the absolute volume of the MgO sample at high pressure allows quantifying its density if the MgO density at a reference pressure is known. The density of MgO at high pressure calculated from our P–V data [Fig. 4(a)] is in agreement with the EOS of Tange *et al.*[29] within ~1%, better than the ~3% error in density estimated by Lobanov *et al.*[2] Overall, our density data confirm that optical measurements of sample area and thickness are able to constrain the evolution of the density of transparent samples upon compression up to ~140 GPa.[2] We note that the here used threshold value for A measurements is different than the one in the supplementary of Lobanov *et al.*,[2] because of different illumination settings and opposite definition (0 or 255) of black/white in the used software.

We derive the Gladstone–Dale relation,[48] fitted to the refractive index data above 20 GPa, using the following parameters: $n = -0.0234 \times \rho + 1.8137$ (uncertainty in $n \sim 1.5\%$), where ρ is the pressure-dependent density in g/cm^3. Based on our refractive index data and the EOS of MgO,[29] we calculated the Lorenz–Lorentz polarizability, α_{LL}, as

$$\alpha_{LL} = \frac{3M(n^2-1)}{\rho 4\pi(n^2+2)}, \quad (4)$$

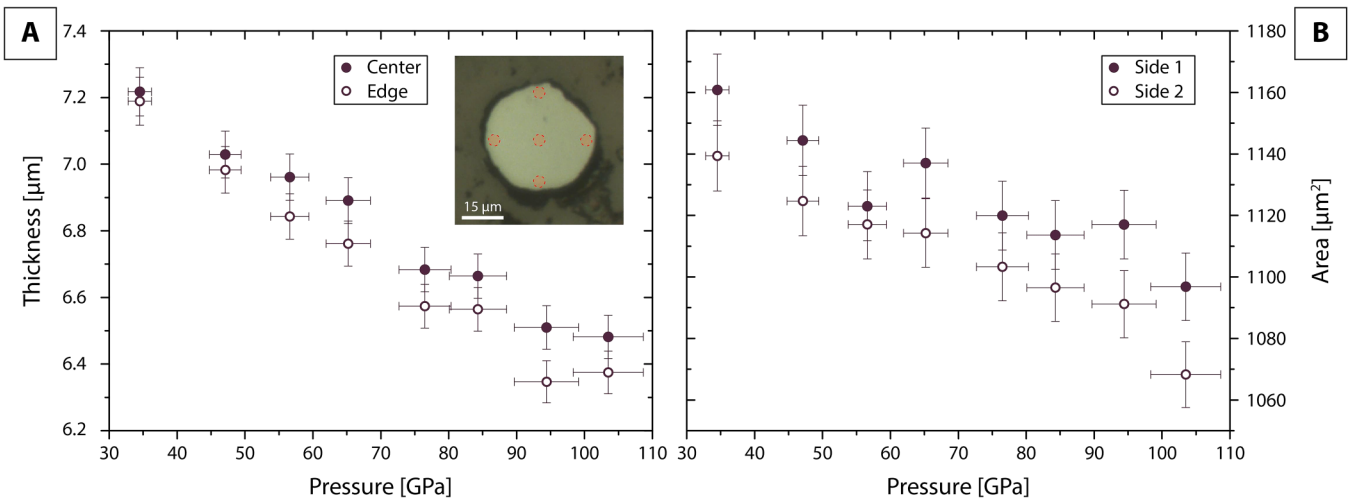

FIG. 3. Measured MgO geometry upon compression in run 4 (300/100 μm culet). (a) Sample thickness at the center and periphery of the DAC cavity (the average of four measurements ~5 μm away from the gasket edge). Inset: optical image of the MgO sample at 24.9 GPa with approximate positions of thickness measurements). (b) Sample area measured from two sides of the DAC.

where we inserted the molar weight of MgO (M) (40.3044 g/mol), the pressure-dependent density (ρ) calculated from MgO EOS[29] and refractive index (n). Propagating the uncertainties for ρ[49] (1%) and for n (1%), the relative error on α_{LL} is 2%. The non-linear behavior of α_{LL} as a function of pressure is due to its inverse-proportional relationship with density in Lorenz–Lorentz formula, and on the intrinsic non-linear behavior of the refractive index as a function of pressure. The model value of α_{LL} obtained from the density (and pressure) dependence of n using the Gladstone–Dale relation well reproduces the full set of calculated α_{LL} [see Fig. 4(b)].

In one of the runs (run 4), we measured the dispersion of the refractive index of MgO, which decreases upon compression by ~28% [Fig. 5(a)], with $\Delta n_{550-870\text{nm}}$ being reduced by ~0.004 from ~0.015 at 1 atm to ~0.011 ($\pm 8.04 \times 10^{-4}$) at ~103 GPa [Fig. 5(b)]. Qualitatively, the nearly pressure-independent index at 600 nm and the decrease in index dispersion suggest that the

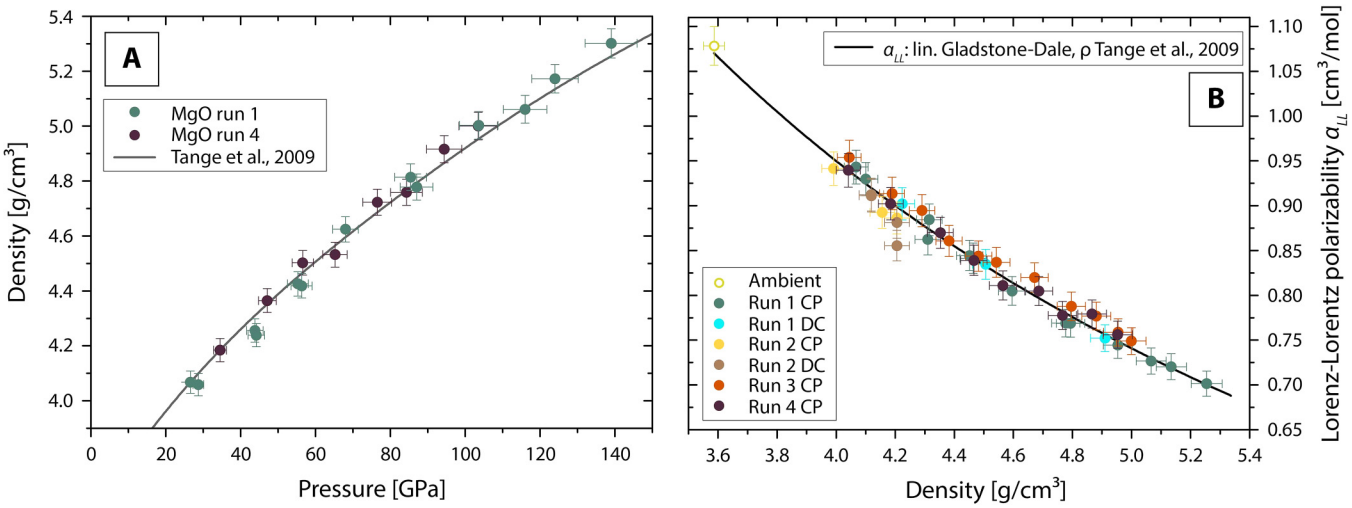

FIG. 4. (a) MgO density measured in this work (circles) compared to data from Tange *et al.*[29] Reference pressures/densities are 26.6 GPa (run 1) and 34.5 GPa (run 4). (b) Lorenz–Lorentz polarizability [α_{LL}, Eq. (4)] evaluated using experimental n and ρ from Tange *et al.*,[29] black line is α_{LL} calculated from the linear Gladstone–Dale relationship of ρ[29] and n to $P \geq 20$ GPa (i.e., $\rho \geq 3.96$ g/cm^3).

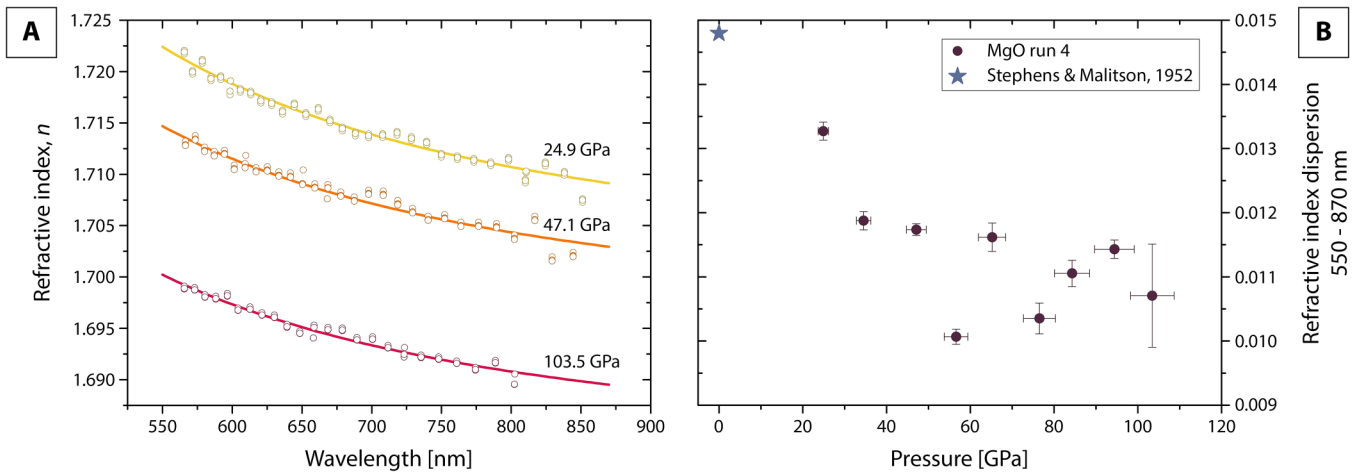

FIG. 5. Wemple–DiDomenico best fits to the experimental dispersion of the refractive index of MgO run 4 at selected pressures (a) and plotted as the difference between measured refractive indices at 550 and 870 nm (b).

valence-to-conduction band energy separation (bandgap) is increasing with pressure. One way to quantify the bandgap is to analyze the index dispersion by the single-effective-oscillator model of Wemple and DiDomenico.[3] In this model, the wavelength dependence of the refractive index is related to two fitting parameters E_0 and E_d, which describe the single oscillator energy and dispersion energy (in eV),

$$n(\lambda) = \sqrt{\frac{E_d E_0}{E_0^2 - \left(\frac{hc}{\lambda}\right)^2} + 1}. \quad (5)$$

Here, h is Planck's constant in eV s and c is the speed of light in m/s, and λ is the wavelength in m. Empirically, E_d is related to the chemical bonding environment (e.g., cation coordination number) and the distribution of charge around the anion (i.e., bonding character), while E_0 is related to the average valence-to-conduction band energy separation.[3,50]

Fitting the single-effective-oscillator model of Wemple and DiDomenico[3] [Eq. (4)] to our wavelength-dispersion data, we find E_0 and E_d for the studied pressure range [Fig. 1(d)]. E_d increases from ∼21.6 eV (1 atm) to ∼23.2 (±0.9) eV at ∼103.5 GPa. The slight increase in E_d with pressure may indicate modest charge redistribution around oxygen. Using the empirical relationship that the oscillator energy E_0 is approximately 1.5 times greater than the optical gap,[3] we experimentally constrain the bandgap of MgO. E_0/1.5 increases by ∼1 eV from 7.4 eV at 1 atm[41] to 8.5 (±0.6) at 103 GPa (Fig. 6). A pressure-induced increase of the bandgap in MgO is consistent with most DFT calculations in the literature.[51–54] However, DFT studies generally show a lower gap energy and a stronger effect of pressure on the increasing bandgap energy.

IV. DISCUSSION

At ambient pressure, our refractive index measurement (without using a DAC) is in agreement with existing experimental data (e.g., Stephens and Malitson).[41] The overall decrease in the refractive index with pressure is consistent with DFT computations[30] and shockwave experiments.[31] Even though diamond cupping produces non-parallelism of the culet faces, we note that a small beam diameter as used here still allows reliable refractive index

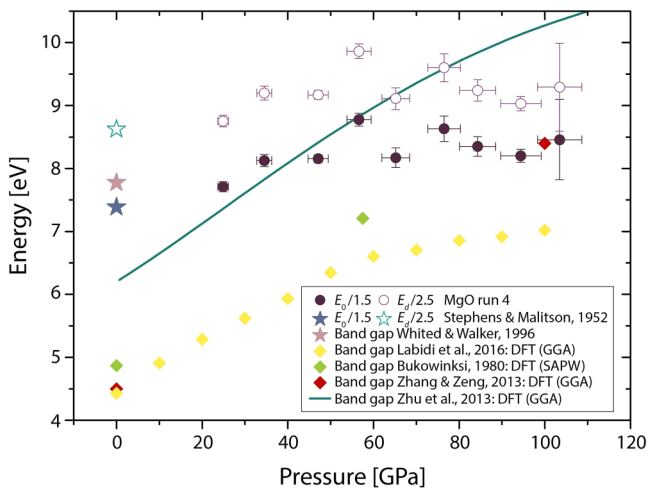

FIG. 6. Results of the Wemple and DiDomenico[3] fit (here E_0/1.5) to the dispersion of the measured index of MgO (circles). The (experimental) data at 1 atm are from Stephens and Malitson[41] (blue star) and Whited and Walker[55] (pink star). In addition, we show calculations from the literature for the bandgap in MgO (green line and diamonds).[51–54] GGA, Generalized gradient approximation; SAPW, symmetrized augmented plane wave.

measurements at the center of the culet, consistent with the results of van Straaten and Silvera[34] who found that the cupping only affects the fringes contrast and not the total reflected signal. However, earlier experimental reports at P <23 GPa show a steeper decrease with P. Vedam and Schmidt[32] found that the index of MgO at 589.3 nm decreases with P by -1.58×10^{-3}/GPa up to 0.7 GPa. Similarly, Balzaretti and Da Jornada[33] found n at 697 nm to decrease by -1.21×10^{-3}/GPa at a maximum P of 10 GPa. In their shockwave experiments, Stevens *et al.*[16] used the density dependence of n and (indirectly) derived a decrease of n by -1.19×10^{-3}/GPa at 532 nm up to ~23 GPa. It is likely that the ~1% relative uncertainty in the refractive index at 600 nm reported here does not allow resolving the stronger dependence of the index on P at $P < 30$ GPa. The general trend of n decreasing on compression is due to a decreasing electronic polarizability, counterbalancing the increase of density with pressure (Fig. 4).

In our refractive index measurements, we assumed a constant refractive index for diamond. According to Katagiri *et al.*,[47] however, uniaxial shock-compression of diamond to 140 GPa (4.2 g/cm^3) increases its refractive index at 532 nm by ~2% (elastic limit). Assuming $n_{dia} = 2.47$ at 140 GPa (elastic limit), we derive $n_{\mathrm{MgO}} = 1.736$ (±0.017), that is 2% higher than $n_{\mathrm{MgO}} = 1.699$ obtained assuming a stress-independent index of diamond ($n_{dia} = 2.418$). We note, however, that within their propagated 1σ uncertainty, Katagiri *et al.*[47] cannot exclude that n_{dia} is constant up to 129 GPa. In addition, such an upward revision in the index of MgO is not justified because it would imply that the refractive index of MgO is constant at $P = 0$–140 GPa, inconsistent with earlier shockwave measurements and theoretical computations that show that the index of MgO decreases with pressure (Fig. 2). Other reports[46,56] on the high-pressure behavior of diamond refractive index suggested that it decreases by up to 5% upon compression to 140 GPa: $n_{dia} = 2.3$. Using this value to analyze the reflectivity of the diamond–MgO interface, we obtain $n_{\mathrm{MgO}} = 1.617$ (±0.016), again inconsistent with the shockwave[31] and DFT data[30] (Fig. 2). Katagiri *et al.*[47] discussed that the response of diamond refractive index to pressure is a function of deformation conditions, which are likely different in diamond anvil cells ($\frac{dn_{dia}}{dP} < 0$)[56] and shockwave experiments ($\frac{dn_{dia}}{dP} > 0$).[47] This interpretation is supported by the DFT computations of Surh *et al.*[46] who found that $\frac{dn_{dia}}{dP}$ is negative upon hydrostatic compression but may be both positive and negative upon uniaxial compression (depending on the principal strain direction). Because the complex deformation regime of the diamond anvil tip results in its non-isotropic optical behavior (birefringence) at high pressure, it is possible that the net effect is that n_{dia} is essentially pressure independent. However, we cannot rule out that the assumption of $n_{dia} = constant$ in our work contributes a systematic error that at 140 GPa exceeds the empirically estimated error of ±1%, despite this assumption providing optimal agreement with independent shockwave data on n_{MgO}, theoretical computations, as well as its pressure–density data. Therefore, we provide tabulated reflectivity data for the diamond–MgO interface in the supplementary material, which can be easily reanalyzed using the Fresnel equation [Eq. (1)]. We maintain, however, that the cases of H_2O and SiO_2 glass constitute indirect justification that the assumption $n_{dia} = \mathrm{constant}$ is reasonable because the pressure–density data for these materials are reproduced.[2,35] A change in n_{dia} by ±2%–5% (as discussed above) would result in the proportional under/over estimation of sample thickness and, thus, pay a ±2%–5% systematic error in the sample density, which is not the case in H_2O[35] and SiO_2 glass,[2] nor it is the case in the present study on MgO.

The continuous decrease in index dispersion of MgO at 550–870 nm ($\Delta n_{550-870\mathrm{nm}}$) is noteworthy, as it indicates an ongoing change in the electronic structure near the valence band maximum and conduction band minimum. The bandgap of MgO at 1 atm is ~7.8 eV based on the reflectance measurements in the UV and VIS ranges.[55,57] These bandgap estimates are also consistent with independent determinations from reflection electron energy loss spectroscopy that yielded ~7.8 eV.[58] The Wemple and DiDomenico[3] fit to the refractive index spectrum at 1 atm[41] yields $E_0/1.5 = 7.4$ eV, broadly consistent with the MgO bandgap reported in the literature. This lends support to the $E_0/1.5$ empirical relation, although this ratio is certainly not universal.[59–61] In the absence of direct measurements of the bandgap of MgO at high pressure, $E_0/1.5$ provides a convenient and semi-quantitative mean of constraining the bandgap of MgO.

To our knowledge, the here shown results (Fig. 6) represent the first experimental high-pressure constraint on the optical bandgap of MgO. Specifically, we observe an opening of the bandgap in MgO from 7.8 eV[55] at 1 atm by ~1 eV upon compression to 103 GPa. The opening is related to a shift of the conduction band toward higher energies, whereas the valence bands are almost insensitive to pressure.[53] The bandgap of MgO at high pressure inferred in this work is higher by ~3 eV than the results of most DFT calculations, likely due to the underestimation of the bandgap by DFT.[45,62]

We constrain how the geometry of a MgO DAC sample (100 μm) evolves on compression up to >100 GPa (Fig. 3). Generally, a cupping of the diamonds is expected in almost all DAC experiments, resulting in a thinner sample away from its center. Li *et al.*[42] reports cupping at pressures as low as 10 GPa, which is consistent with our measurements that readily resolve cupping at $P \sim 30$ GPa. Future DAC experiments can use the pressure dependence of the refractive index to quantify sample thicknesses by white light interferometric measurements. This is directly relevant for radiative and lattice thermal conductivity measurements where sample thickness is crucial for getting accurate results. The pressure dependence of the refractive index found here can be used to calculate the radiative conductivity[4] of (Mg,Fe)O samples at high pressure under the assumption that the addition of moderate amounts of iron in substitution of Mg does not change the pressure dependence of the refractive index. The extension of the 600 nm refractive index of MgO up to 140 GPa can also be beneficial for shockwave experiments using MgO as an interferometer window material, since previous studies in the VIS range are only limited to <23 GPa.[16]

Because of the uniaxial stress conditions present in the DAC sample chamber, radial strain and radial pressure gradients could be strong. However, we were not able to reliably resolve pressure gradients across the studied sample within the accuracy of the pressure determination method (5%).[37] Also, given the slight changes in n with P, small pressure gradients will have no measurable effect on the derived sample thickness and density. We are able to

reproduce the pressure-dependent density within 1% with respect to the published EOS of MgO (300 K) by Tange *et al.*[29] Overall, the agreement between the pressure–volume data measured here and that expected from the MgO EOS within ∼1% confirms the applicability of the optical determination of sample density,[2,34,35] which could be beneficial for high-pressure studies of non-crystalline materials.

V. CONCLUSIONS

We presented the evolution of the refractive index of MgO at 600 nm up to ∼140 GPa. With the pressure dependence of the refractive index, we demonstrate a reliable way to accurately determine thicknesses by the analysis of interference fringe distances which can be applied to any DAC experiment using MgO as a sample or pressure transmitting medium. We show that simple and straightforward in-house DAC experiments can help to derive sample densities at pressures >1 Mbar. Even though the error of this kind of measurement is certainly larger compared to synchrotron based techniques (<0.1%,[63] for crystalline materials), it provides reliable estimations of the densification trend if the density at one reference pressure is known. We also experimentally constrained the pressure dependence of the bandgap for MgO and show that it opens by ∼1 eV over a 100 GPa range, considerably less than what is expected from DFT calculations. This implies that over the whole pressure range of the Earth's lower mantle, pressure has only minor effects on the electrical conductivity of MgO.

SUPPLEMENTARY MATERIAL

See the supplementary material for the measured reflectivity values of the diamond–MgO interface.

ACKNOWLEDGMENTS

This work was supported by the Helmholtz Young Investigators Group CLEAR (No. VH-NG-1325). We thank two anonymous reviewers for their constructive criticism and suggestions that helped us improve this manuscript.

AUTHOR DECLARATIONS

Conflict of Interest

The authors have no conflicts to disclose.

Author Contributions

Lukas Schifferle: Data curation (equal); Formal analysis (equal); Investigation (equal); Methodology (equal); Software (equal); Validation (equal); Visualization (equal); Writing – original draft (lead). **Sergio Speziale:** Conceptualization (equal); Formal analysis (supporting); Methodology (equal); Resources (equal); Writing – original draft (equal). **Sergey S. Lobanov:** Conceptualization (equal); Data curation (equal); Funding acquisition (lead); Investigation (equal); Methodology (equal); Software (equal); Supervision (lead); Writing – original draft (equal).

DATA AVAILABILITY

The data that support the findings of this study are available from the corresponding author upon reasonable request.

REFERENCES

[1]P. Hervé and L. Vandamme, Infrared Phys. Technol. **35**, 609–615 (1994).
[2]S. S. Lobanov, S. Speziale, B. Winkler, V. Milman, K. Refson, and L. Schifferle, Phys. Rev. Lett. **128**, 77403 (2022).
[3]S. H. Wemple and M. DiDomenico, Phys. Rev. B **3**, 1338–1351 (1971).
[4]S. P. Clark, Trans. Am. Geophys. Union **38**, 931 (1957).
[5]C. J. Grose and J. C. Afonso, Geochem. Geophys. Geosyst. **20**, 2378–2394 (2019).
[6]A. F. Goncharov, S. S. Lobanov, X. Tan, G. T. Hohensee, D. G. Cahill, J.-F. Lin, S.-M. Thomas, T. Okuchi, and N. Tomioka, Phys. Earth Planet. Inter. **247**, 11–16 (2015).
[7]H. Keppler, L. S. Dubrovinsky, O. Narygina, and I. Kantor, Science **322**, 1529–1532 (2008).
[8]S. S. Lobanov, N. Holtgrewe, J.-F. Lin, and A. F. Goncharov, Earth Planet. Sci. Lett. **479**, 43–49 (2017).
[9]S. S. Lobanov, N. Holtgrewe, G. Ito, J. Badro, H. Piet, F. Nabiei, J.-F. Lin, L. Bayarjargal, R. Wirth, A. Schreiber, and A. F. Goncharov, Earth Planet. Sci. Lett. **537**, 116176 (2020).
[10]S. S. Lobanov, F. Soubiran, N. Holtgrewe, J. Badro, J.-F. Lin, and A. F. Goncharov, Earth Planet. Sci. Lett. **562**, 116871 (2021).
[11]M. Murakami, A. F. Goncharov, N. Miyajima, D. Yamazaki, and N. Holtgrewe, Earth Planet. Sci. Lett. **578**, 117329 (2022).
[12]Z. Konôpková, R. S. McWilliams, N. Gómez-Pérez, and A. F. Goncharov, Nature **534**, 99–101 (2016).
[13]K. Ohta, Y. Kuwayama, K. Hirose, K. Shimizu, and Y. Ohishi, Nature **534**, 95–98 (2016).
[14]Z. M. Geballe, N. Sime, J. Badro, P. E. van Keken, and A. F. Goncharov, Earth Planet. Sci. Lett. **536**, 116161 (2020).
[15]Y. Okuda, K. Ohta, A. Hasegawa, T. Yagi, K. Hirose, S. I. Kawaguchi, and Y. Ohishi, Earth Planet. Sci. Lett. **547**, 116466 (2020).
[16]R. E. Setchell, "Index of refraction of shockcompressed fused silica and sapphire," J. Appl. Phys. **50**, 8186–8192 (1979).
[17]M. A. Shand, *The Chemistry and Technology of Magnesia* (Wiley-Interscience, Hoboken, NJ, 2010).
[18]R. S. McWilliams, D. K. Spaulding, J. H. Eggert, P. M. Celliers, D. G. Hicks, R. F. Smith, G. W. Collins, and R. Jeanloz, Science **338**, 1330–1333 (2012).
[19]R. Musella, S. Mazevet, and F. Guyot, Phys. Rev. B **99**, 064110 (2019).
[20]W. M. Haynes, *CRC Handbook of Chemistry and Physics*, 97th ed. (CRC Press, 2016).
[21]I. O. Wilson, IEEE Proc., Part A: Phys. Sci., Meas. Instrum., Manage. Educ. Rev. UK **128**, 159 (1981).
[22]A. B. Belonoshko, S. Arapan, R. Martonak, and A. Rosengren, Phys. Rev. B **81**, 054110 (2010).
[23]F. Soubiran and B. Militzer, Phys. Rev. Lett. **125**, 175701 (2020).
[24]F. Coppari, R. F. Smith, J. Wang, M. Millot, D. Kim, J. R. Rygg, S. Hamel, J. H. Eggert, and T. S. Duffy, Nat. Geosci. **14**, 121–126 (2021).
[25]A. Onodera, K. Suito, and N. Kawai, J. Appl. Phys. **51**, 315–318 (1980).
[26]W. R. Panero and R. Jeanloz, "The effect of sample thickness and insulation layers on the temperature distribution in the laser-heated diamond cell," Review of Scientific Instruments **72**, 1306–1308 (2001).
[27]J. S. Pigott, D. M. Reaman, and W. R. Panero, "Microfabrication of controlled-geometry samples for the laser-heated diamond-anvil cell using focused ion beam technology," Review of Scientific Instruments **82**, 115106 (2011).
[28]S. M. Dorfman, V. B. Prakapenka, Y. Meng, and T. S. Duffy, J. Geophys. Res. **117**, B08210 (2012).
[29]Y. Tange, Y. Nishihara, and T. Tsuchiya, J. Geophys. Res. **114**, B03208 (2009).
[30]A. R. Oganov, M. J. Gillan, and G. D. Price, J. Chem. Phys. **118**, 10174–10182 (2003).

[31]D. E. Fratanduono, J. H. Eggert, M. C. Akin, R. Chau, and N. C. Holmes, J. Appl. Phys. **114**, 043518 (2013).
[32]K. Vedam and E. D. D. Schmidt, Phys. Rev. **146**, 548–554 (1966).
[33]N. M. Balzaretti and J. A. H. Da Jornada, High Pressure Res. **2**, 183–191 (1990).
[34]J. van Straaten and I. F. Silvera, Phys. Rev. B: Condens. Matter **37**, 1989–2000 (1988).
[35]C.-S. Zha, R. J. Hemley, S. A. Gramsch, H.-K. Mao, and W. A. Bassett, J. Chem. Phys. **126**, 074506 (2007).
[36]Y.-J. Kim, P. M. Celliers, J. H. Eggert, A. Lazicki, and M. Millot, Sci. Rep. **11**, 5610 (2021).
[37]Y. Akahama and H. Kawamura, J. Appl. Phys. **100**, 043516 (2006).
[38]S. S. Lobanov, L. Schifferle, and R. Schulz, Rev. Sci. Instrum. **91**, 053103 (2020).
[39]S. van der Walt, S. C. Colbert, and G. Varoquaux, Comput. Sci. Eng. **13**, 22–30 (2011).
[40]A. Meurer, C. P. Smith, M. Paprocki, O. Čertík, S. B. Kirpichev, M. Rocklin, A. Kumar, S. Ivanov, J. K. Moore, S. Singh, T. Rathnayake, S. Vig, B. E. Granger, R. P. Muller, F. Bonazzi, H. Gupta, S. Vats, F. Johansson, F. Pedregosa, M. J. Curry, A. R. Terrel, Š Roučka, A. Saboo, I. Fernando, S. Kulal, R. Cimrman, and A. Scopatz, Peer J. Comput. Sci. **3**, e103 (2017).
[41]R. E. Stephens and I. H. Malitson, J. Res. Natl. Bur. Stand. **49**, 249–252 (1952).
[42]B. Li, C. Ji, W. Yang, J. Wang, K. Yang, R. Xu, W. Liu, Z. Cai, J. Chen, and H.-K. Mao, Proc. Natl. Acad. Sci. U.S.A. **115**, 1713–1717 (2018).
[43]R. J. Hemley, H.-K. Mao, G. Shen, J. Badro, P. Gillet, M. Hanfland, and D. Häusermann, Science **276**, 1242–1245 (1997).
[44]M. D. Abramoff, P. J. Magalhaes, and S. J. Ram, Biophotonics Int. **11**, 36–42 (2004).
[45]Á Morales-García, R. Valero, and F. Illas, J. Phys. Chem. C **121**, 18862–18866 (2017).
[46]M. P. Surh, S. G. Louie, and M. L. Cohen, Phys. Rev. B: Condens. Matter **45**, 8239–8247 (1992).
[47]K. Katagiri, N. Ozaki, K. Miyanishi, N. Kamimura, Y. Umeda, T. Sano, T. Sekine, and R. Kodama, Phys. Rev. B **101**, 184106 (2020).
[48]J. H. Gladstone and T. P. Dale, Philos. Trans. R. Soc. **153**, 317–343 (1863).
[49]L. Liu and Y. Bi, MRE **1**, 224–236 (2016).
[50]S. H. Wemple and M. DiDomenico, Phys. Rev. Lett. **23**, 1156–1160 (1969).
[51]S. Labidi, J. Zeroual, M. Labidi, K. Klaa, and R. Bensalem, Solid State Phenom. **257**, 123–126 (2016).
[52]M. S. T. Bukowinski, J. Geophys. Res. **85**, 285–292 (1980).
[53]J. Zhang and Z. Zeng, Int. J. Mod. Phys. C **24**, 1350052 (2013).
[54]Q. Zhu, A. R. Oganov, and A. O. Lyakhov, Phys. Chem. Chem. Phys. **15**, 7696–7700 (2013).
[55]R. C. Whited and W. C. Walker, Phys. Rev. Lett. **22**, 1428–1430 (1969).
[56]M. I. Eremets, V. V. Struzhkin, J. A. Timofeev, I. A. Trojan, A. N. Utjuzh, and A. M. Shirokov, High Pressure Res. **9**, 347–350 (1992).
[57]D. M. Roessler and W. C. Walker, Phys. Rev. **159**, 733–738 (1967).
[58]S. Heo, E. Cho, H.-I. Lee, G. S. Park, H. J. Kang, T. Nagatomi, P. Choi, and B.-D. Choi, AIP Adv. **5**, 077167 (2015).
[59]I. P. Studenyak, S. M. Bereznyuk, M. M. Pop, V. I. Studenyak, A. I. Pogodin, O. P. Kokhan, B. Grančič, and P. Kúš, Semicond. Phys. Quantum Electron. Optoelectron. **23**, 186–192 (2020).
[60]A. M. Alsaad, Q. M. Al-Bataineh, A. A. Ahmad, Z. Albataineh, and A. Telfah, Optik **211**, 164641 (2020).
[61]K. Tanaka, Thin Solid Films **66**, 271–279 (1980).
[62]B. Winkler and V. Milman, Z. Kristallogr. Cryst. Mater. **229**, 112 (2014).
[63]K. Hirose, N. Sata, T. Komabayashi, and Y. Ohishi, Phys. Earth Planet. Inter. **167**, 149–154 (2008).